Digest Journal of Nanomaterials and Biostructures, Vol. 2, No. 2, June 2007, p. 221 - 241

LASER ABLATION OF CRYOGENIC FILMS: IMPLICATIONS TO MATRIX-ASSISTED PULSED LASER DEPOSITION OF BIOPOLYMERS AND DEDICATED APPLICATIONS IN NANOTECHNOLOGY

Olga Kokkinaki, Savas Georgiou*

Institute of Electronic Structure and Laser, Foundation for Research and Technology – Hellas, 71110, Heraklion, Crete, Greece

Matrix-Assisted-Pulsed Laser- Evaporation (MAPLE) is evolving into a powerful technique for the controlled deposition of biopolymers. The method relies on the finding that the biopolymers dissolved within a frozen, absorbing solvent can, upon laser irradiation, eject in the gas phase in intact and functional form. For the better mechanistic understanding and optimization of the technique, we review here studies on laser-induced material ejection from cryogenic solids of simple molecular/ organic compounds. It is demonstrated that at low laser fluences, thermal desorption dominates, so that, only weakly-bound-to-the-solvent dopants/ solutes desorb. However, above a specific fluence, a different mechanism becomes operative, resulting in the unselective ejection of a layer of material (ablation). Ejection of solutes that are strongly bound to the solvent e.g. of biopolymers, can take place only in this regime. Therefore, the term evaporation in MAPLE acronym (and "desorption" in MALDI) are inappropriate. At least for photoinert compounds and nanosecond laser pulses, ablation is shown to be due to explosive boiling. We discuss the implications of this mechanism for MAPLE. Chemical effects in UV ablation of frozen compounds are reviewed and conditions for their minimization are presented. Finally, besides their mechanistic interest, the studies can also yield information on a number of issues relevant to nanotechnology.

(Received May 18, 2007; accepted May 25, 2007)

Keywords: As_2S_3, Laser ablation, Cryogenic films, Biopolymers, Nanotechnology

1. Introduction

Ever since its discovery, laser ablation has constituted the basis of powerful techniques [1] in a wide spectrum of applications, ranging from polymer structuring in microelectronics [2] to polymer/ biopolymer characterization in analytical chemistry (Matrix-Assisted-Laser-Desorption-Ionization of biopolymers, MALDI) [[3]-[6]], to tissue excision in medicine [7] and conservation of painted artworks [8]. In particular, Pulsed Laser Deposition (PLD) [9] -which schematically entails the deposition of the material/ plume that is ejected from an irradiated target onto a substrate placed in the path of its ejection - enables the growth of films/ coatings of few 100s nm of a wide range of materials with a high degree of control of the thickness and of the morphological characteristics. Such films/ coatings have found uses in devices in micro/ optoelectronics [[5], [9], [10]], bio/chemical sensors [11], systems for drug delivery [12] or aiming at improving biocompatibility of devices [[13]-[15]].

"Matrix Assisted Pulsed Laser Evaporation" (MAPLE) is a variation of PLD and was introduced [16] in order to face the challenge of depositing organic/ polymeric materials with minimal thermal or chemical decomposition. To this end, in MAPLE, the polymers/ biomolecules are dissolved in an absorbing frozen solvent, instead of being directly irradiated in the bulk [[17]-[19]]. Because the laser energy is absorbed mainly by the solvent/ matrix and not by the polymer, the "violent nature" of laser interaction may be largely reduced (at least, deleterious photochemical modifications to the polymer). This idea was introduced by analogy to the MALDI studies [[6], [20]] that had demonstrated that through dissolution of biopolymers within specific, highly absorbing organic matrices/ crystals, laser-induced ejection of biopolymers may be effected with

*Corresponding author: sgeorgiu@iesl.forth.gr

minimal fragmentation, thereby enabling their mass spectroscopic characterization. However, the matrices employed in MALDI are chemically complex, so that they do not offer any advantages for deposition applications. The development of MAPLE relied on the realization that the effectiveness for the ejection (and subsequent deposition) of biopolymers in an intact form is not restricted to the specific matrices employed in MALDI, but it may be effected upon irradiation of polymers and biopolymers dispersed within simple absorbing systems (solvents). Since biopolymers are usually employed within an aqueous solution, freezing of the sample can provide an easily "manipulated" solid target. The studies thus far have clearly demonstrated [[21]-[27]] the potential of MAPLE for the deposition of a wide range of organic macromolecules (e.g. carbohydrates [16], nanotubes), polymers/ biopolymers (e.g. PolyEthyleneGlycol) or even of larger biological structures (e.g. viruses, proteins, cells, tissue components) in intact and functional form. Recently, films of polysaccharides [23], blood and mussel proteins [[24]- [26]] (Figure 1) as well as collagen [27] were successfully produced for drug delivery and diagnostic applications. Thus, this method provides the possibility for the fabrication of micro/ nano arrays of biomaterials [[28]-[30]] with applications in biosensing, chemical sensing, biochemical/ microbiological analysis and even for therapeutic purposes (drug delivery systems, implant/ prosthetic fabrication).

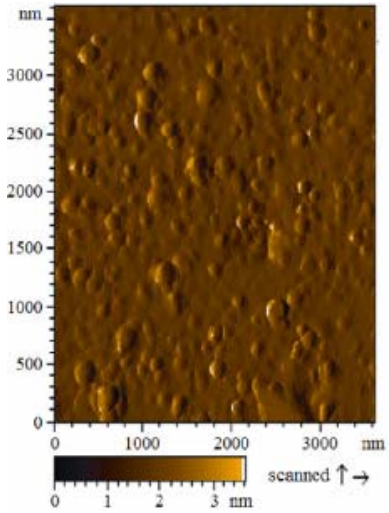

Fig. 1. High-resolution topography flattened atomic force micrograph of matrix assisted laser evaporation-deposited *Mytilus edulis* foot protein-1 film (reprinted from ref. [24] with permission).

Although the effectiveness of MAPLE has improved substantially over the last years, a general enough experimental protocol(s) for the deposition of a variety of polymers/ biomolecules remains to be established. This difficulty can be partly ascribed to the wide range and to the high chemical and structural complexity of materials to be deposited. However, the major difficulties seem to relate to the laser irradiation parameters (wavelength, fluence, pulse width- though the last parameter has not been particularly examined) affecting the quality of deposit. In addition, the choice of the matrix is also critical for the success of the technique. Understandably, one criterion is the photochemical inertness of the matrix so that chemical reactions with the polymer/analyte are minimized. The studies indicate that in addition best results are obtained for relatively volatile matrices with a low concentration of homogeneously dissolved/ dispersed polymer. These features appear intuitively reasonable, but until attaining a detailed justification, they represent important, but only phenomenological, criteria. Other factors relating to the frozen target that may affect the efficiency/ effectiveness of MAPLE include the matrix structure (i.e. amorphous, crystalline), degree of solubility or dispersal of the analyte and its conformational stabilization within the target, etc. Of course, there are a number of issues/ requirements relating to the deposition process itself, but these requirements will not be specifically addressed in this review.

For the optimization of MAPLE, a closer examination of the ejection process is necessary, as it is the first step in the procedure and probably the determining factor for its success. Mechanistic understanding of the ejection process has been quite limited. Often, a simple

photothermal mechanism has been suggested [21] to operate (as also indicated by the term "evaporation" in the MAPLE acronym). According to this model, the laser energy absorbed by the matrix (frozen solvent) is converted into thermal, which causes the vaporization of the matrix. Upon vaporization, the polymers, presumably through collisions with the desorbing matrix molecules, attain sufficient kinetic energy to be ejected to the gas phase. Though a thermal mechanism seems to explain why best results in MAPLE are obtained with volatile solvents, it fails to account for several other observations. In addition, it is difficult to accept that simple collisions with the solvent molecules can accelerate the large (massy) biopolymers to ejection. In cases that the absorbed energy seems to be too low to effect thermal desorption/ evaporation, the ejection process is suggested to be due to a photomechanical (spallation) mechanism. For typical excimer nanosecond laser pulses (τ_p~30 ns). This is a likely mechanism for thin films cast on substrates of very different acoustic impendances [31], but as discussed in Section 4a, it is likely not dominant in the irradiation of thick frozen solids.

Alternatively, the explosive-boiling model has been advanced on the basis of the Molecular Dynamics (MD) simulations [32] and thermodynamic considerations [33]. MD simulations, relying on a "breathing sphere" representation of the particles of the substrate, predict that below a well-defined fluence (threshold), desorption is molecular (consistent with surface vaporization), whereas above this fluence, massive ejection of material occurs largely in the form of clusters. According to thermodynamic considerations, boiling is too slow to be of importance on nanoseconds-microseconds timescales. As a result, with increasing laser fluence, the system is overheated to higher and higher temperatures, until violent boiling ("explosive boiling) occurs, with the system ejected into a mixture of gas and droplets. However, adoption of this model in MAPLE studies has been rather limited. A common argument is that the breathing-sphere model is too simple to represent the complexity of the compounds employed in MAPLE studies, and the values employed for a number of parameters (in order to reduce the computational requirements) differ drastically from those of real systems.

Well before the advent of MAPLE, we initiated the study of cryogenic solids for the detailed examination of the processes in laser-organics interactions [34]. This choice was based on the reasoning that elucidation of the involved processes calls for the use of the simplest compounds. However, under ambient conditions, simple organic compounds are generally gaseous or liquid. Thus, for simulating the solid state, we have turned to the study of the van der Waals (cryogenic) solids that are formed by the condensation of vapours of these compounds on low temperature substrates. Given the physicochemical simplicity of these systems, photodesorption/ ejection processes can be probed in detail. Furthermore, the structure of the condensed solids can be varied systematically (e.g. amorphous, glassy or crystalline), thus enabling assessment of its influence on the ejection processes. In addition, there is extensive information available on the photophysics/chemistry of these compounds. Thus, the processes and effects that are involved in photoejection from cryogenic/ frozen films can be accurately and quantitatively evaluated, thus enabling detailed assessment of the mechanisms involved in MAPLE.

In the following, we first examine the features/ characteristics of the laser-induced ejection dynamics from cryogenic films (Section 2). To this end, we review comparative studies of the desorption/ ejection efficiencies in the UV irradiation of frozen solids as a function of laser fluence (F_{LASER}). We show that ejection at high fluences clearly differs from thermal desorption/evaporation; instead, at these fluences, unselective ejection of a layer of material is observed (ablation). The most important conclusion is that ejection of species that are strongly bound to the matrix such as of biopolymers in frozen aqueous matrix can occur *only* in the ablative regime. Other implications of the studies for MALDI and MAPLE are also discussed.

In Section 3, we overview the chemical processes induced in the UV-laser irradiation/ ablation of condensed solids of photo-active compounds. In particular, we emphasize that induction effects in such systems is a significant factor for the correct mechanistic understanding (as well as optimization) of laser processing of cryogenic films/ solids.

Section 4a pertains to the study of the mechanisms that are responsible for the ejection dynamics observed at high fluences (ablation). We show that at least for photoinert compounds/ matrices, explosive boiling is involved (Section 4b). The implications of this mechanism for the understanding and optimization of MAPLE are discussed (Section 5). Besides their importance for MAPLE, our results are of wider relevance for nanoscience/ technology (Section 6). Explosive

boiling involves the nucleation and growth of bubbles on the nm scale. The study of bubble dynamics is fundamental to elucidating thermodynamics and dynamics of condensed phases on the nm scale. Bubble formation can also limit the diagnostic capability of nano-resolved diagnostic techniques and can also be a crucial factor in nanoprocessing/ fabrication. The use of cryogenic solids offers the advantage that bubble dynamics may be examined in detail, free from the problems limiting its study in liquids/ solutions.

2. Examination of ejection dynamics

A common phenomenological description of laser ejection relies on the examination of the etching depth (or ejected amount) as a function of laser fluence. The onset of the sharp increase of the etching depth/ ejected amount is considered to correspond to the threshold fluence for ablation. However, in most cases, the dependence is quite smooth, so that it is both difficult to specify accurately and also questionable if it represents the onset of new processes. For instance, in some MALDI studies, a lower fluence "limit" for the detection of bio-analytes/ proteins in the gas-phase has been ascribed to the existence of a fluence threshold for the ejection of these analytes in the gas-phase; however, several (if not most) studies ascribe this simply to instrumental/ detection limitations (i.e., to the low ion signal of the biopolymers) [35]. In MAPLE studies, there has been very little discussion of the dependence of the ejection efficiency of the biopolymer on laser fluence [21]. In fact, the terms "desorption" and "evaporation" in the MAPLE and MALDI acronyms suggest a simple thermal desorption process.

Several studies rely on the examination of the desorbate translational distributions **Eroare! Fără sursă de referință.** for obtaining information on the photo-ejection processes. However, the desorbate translational distributions may be severely modified by post-desorption collisions (important even for desorption of 0.1 monolayers [37]). Widely different interpretations have been proposed, in terms of thermal/ non-thermal mechanisms, 'hyper-thermal' vs. 'near-thermal' desorption. Generally, a bi-modal distribution is observed, with a very high velocity (~ 1 eV most probable value) component and a much slower one. Therefore, though of importance for deposition processes, the characteristics of the translational distributions may not directly reflect the processes occurring in the substrate that lead to material ejection.

Ideally, for examining if a thermal or other mechanisms are applicable, we would like to examine systems in which all the parameters are kept the same (e.g., absorption coefficient, chemical constitution, etc), with only the binding energy between molecules varied in a systematic way. Of course, in practice, such systems are not available, but the objective can be attained by comparing the dependence of the ejection signals of dopants (dispersed within a matrix) of different binding energy to the matrix (solvent) [[38]-[40]]. To this end, the matrix is always the same and we employ as dopants compounds of increasing size within a homologue series: with increasing size, the number of pairwise additive interactions of the dopant with the matrix increase and, thus, their overall binding to the matrix. To ensure that the absorption coefficient is always the same, the chosen dopants do not absorb at the irradiation wavelength (248 nm), so that absorption is exclusively by the matrix and in all cases the dopant-to-matrix molar ratio is the same. Since the excitation/ deactivation processes are the same in the comparison, the relative ejection signals of the dopants provide direct information on the nature of the energy dissipation in the substrate and on the mechanisms of material ejection. For a thermal process, the desorption intensities of the dopants should correlate with their binding energy to the matrix. On the other hand, no such correlation should be observed for mechanisms such as photomechanical or photochemical.

In most of our work, as matrix we employ $C_6H_5CH_3$ (at 248 nm, absorption coefficient ~ 3700 cm^{-1} from in-situ measurements) for three main reasons. First, it is one of the simplest organic molecules and it may be a useful solvent in MAPLE for various hydrophobic compounds/ biopolymers. Second, it presents minimal photo-fragmentation (at 248 nm), thereby avoiding complications due to any photoreactivity. Third, it has been extensively studied, thus the well-defined values permit quantitative analysis of the results. As dopants, we include alkanes (e.g. c-C_3H_6, c-C_6H_{12}, $C_{10}H_{22}$, $C_{15}H_{32}$) and ethers/ alcohols (e.g. $(CH_3)_2(CH_2)_nO$, D_2O, $CH_3(CH_2)_nOH$) which are nearly transparent at 308 nm and 248 nm. Among all the examined dopants, we refer in particular to the results concerning dimethylether ($(CH_3)_2O$) and decane ($C_{10}H_{22}$). Their binding

energies to the $C_6H_5CH_3$ matrix are respectively ~0.4 eV/molecule and ~0.8 eV/molecule, as determined by Thermal Desorption Spectroscopy (for reasons of brevity, we refer to $(CH_3)_2O$ as "volatile", while to $C_{10}H_{22}$ as "non-volatile" dopant). The intensities of the ejecta are probed as a function of laser fluence (F_{LASER}) via quadrupole mass spectrometry (i.e., neutral desorbates are detected by electron-impact ionization). Typical time-of-flight spectra recorded are shown in Fig. 2. The film thickness is ≥ 50 μm, i.e., much larger than the optical penetration depth. Further information on the experimental procedures can be found in Ref. [41].

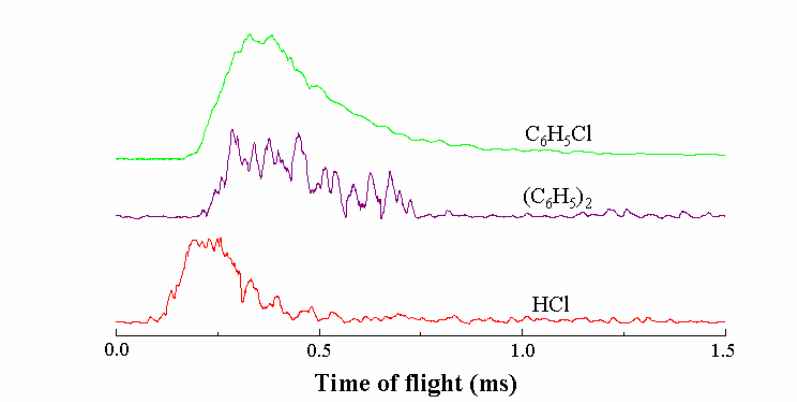

Fig. 2. Time-of-flight spectra of the parent molecule and of the products $(C_6H_5)_2$ and HCl ejected upon irradiation of neat C_6H_5Cl solids at fluence just above the ablation threshold (λ=248 nm).

Considering first the fluence dependence of the ejection from neat frozen $C_6H_5CH_3$ solid, its desorption signal exhibits an exponential dependence on laser fluence (F_{LASER}) (Fig. 3), increasing sharply above ~100 mJ/cm^2. If we assume, as commonly, that Signal scales as $\frac{1}{\alpha}\ln\left(\frac{F_{LASER}}{F_{thr}}\right)$, where α is the absorption coefficient, and plot the data accordingly, the threshold is estimated at 100 ± 10 mJ/cm^2. However, a closer examination of the plot reveals another increase of the desorption intensity at ~ 45 mJ/cm^2 (inset of Fig. 3).

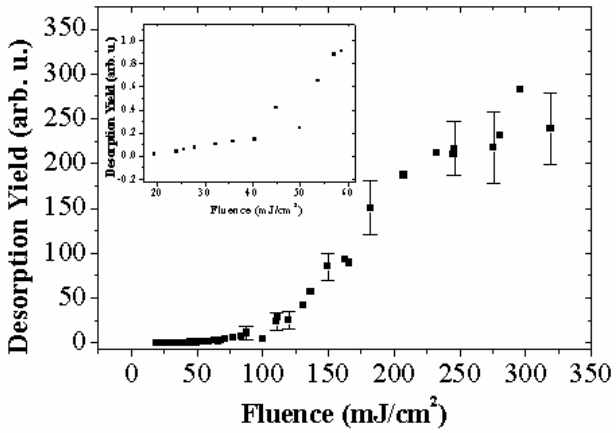

Fig. 3. Intensity of the ejected $C_6H_5CH_3$ recorded from freshly deposited $C_6H_5CH_3$ films as a function of the incident laser fluence (λ=248 nm). The error bars represent 2σ, as determined from at least 6-7 different measurements of each datum point. The inset depicts in detail the intensity at low fluences.

Examination of the ejection intensities of the dopants ($(CH_3)_2O$, C_6H_{12} and $C_{10}H_{22}$) shows that two fluence ranges can be delineated with characteristically different ejection observables/ dynamics (At very low fluences < 5 mJ/cm^2, desorption is very weak, i.e., sub-monolayers and

system-specific. The processes operative at these fluences have been examined in detail by surface scientists [37].):

- At low laser fluences, the signal of the volatile dopants (e.g. $(CH_3)_2O$) is considerably higher than the $C_6H_5CH_3$ signal, even though its molar concentration in the film is 1/5 that of $C_6H_5CH_3$. On the other hand, at these fluences no signal is detected for the non-volatile dopants (e.g. for $C_{10}H_{22}$). Apparently, at low fluences, only dopants that are weakly bound to the matrix desorb. By re-plotting the data in an Arrhenius-type format (i.e., ln(signal) vs. 1/T, where T is the peak (surface) temperature attained upon irradiation $T = T_0 + \frac{\alpha F_{LASER}}{\rho c_p} e^{-\alpha z}$ where T_0=120 ^{0}K, c_p the heat capacity of the condensed $C_6H_5CH_3$ solid (in the case of mixtures c_p is estimated as the molar averaged heat capacities of $C_6H_5CH_3$ and dopant [[42], [43]]), α the absorption coefficient for neat or doped toluene solid and ρ is the molar average molar density. The activation energy for desorption (ΔE_{des}) of the compounds can be determined from the slope of the linear fitting. The activation energies for ejection of the dopants and of toluene are found to agree well with their binding energies to the matrix as determined by Thermal Desorption Spectroscopy (Table 1). Therefore, at these fluences, material ejection is consistent with surface thermal desorption. The conclusion is reinforced by the experimental results described in Section 5 on phase transformations.
- In contrast, at higher fluences, both the weakly and the strongly-bound-to-the-matrix dopants are found to eject in the gas phase. In fact, for all systems, the dopant-to-matrix signal ratios reach values close to the film stoichiometry, although in the case of the strongly bound dopants, deviations are observed (Figure 4) [39]. Clearly, at these fluences, the ejection intensity of the dopants does not correlate with their binding energy to the matrix. For the "nonvolatile" dopants (e.g. $C_{10}H_{22}$), the ejection intensity relatively to that of the matrix remains almost constant with successive laser pulses [40]. Furthermore, the dependence of the "nonvolatile" dopant ejection efficiency on F_{LASER} (> the ablation threshold) is almost identical to that of the matrix (Fig. 5), i.e. for both $C_6H_5CH_3$ and $C_{10}H_{22}$, $S_{ejected} \propto \ln\left(\frac{F_{LASER}}{F_{thr}}\right)$ where $S_{ejected}$ represents the intensity of the corresponding compound and F_{thr} represents the same threshold value. Taken together, these results show that these fluences entail the unselective expulsion of a volume of material, i.e., independently of the binding energy of the dopants. Besides the above, for "volatile" dopants (i.e., dopants desorbing both below and above the ablation threshold) ejection dynamics changes characteristically (e.g. different dependence on laser pulses, different translational distributions, etc).

Table 1. Activation energies derived from TDS and Laser induced desorption.

System	T_{des}[(a)] (^{o}K)	E_{TDS}[(b)] (kJ/mol)	E_{LASER}[(c)] (kJ/mol)
neat $C_6H_5CH_3$	170	41±2	30±3
$(CH_3)_2O$/ $C_6H_5CH_3$	145	16±3	17±5
c-C_3H_6/ $C_6H_5CH_3$	135	15±3	14±5
C_6H_{12}/ $C_6H_5CH_3$	176	33±4	25±5
$C_{10}H_{12}$/ $C_6H_5CH_3$	-	d	77

a) Temperature for the onset of desorption in the TDS experiments. In the case of the binary systems, the temperature refers to the desorption of the dopant.
b) The activation energy for desorption of the compounds as determined from fittings of the rising edge of the TDS curves.
c) Activation energies determined from conventional semilogarithmic plots of the laser-induced desorption signals vs $1/F_{LASER}$.
d) $C_{10}H_{22}$ desorbs thermally at temperatures well above that at which all $C_6H_5CH_3$ has desorbed.

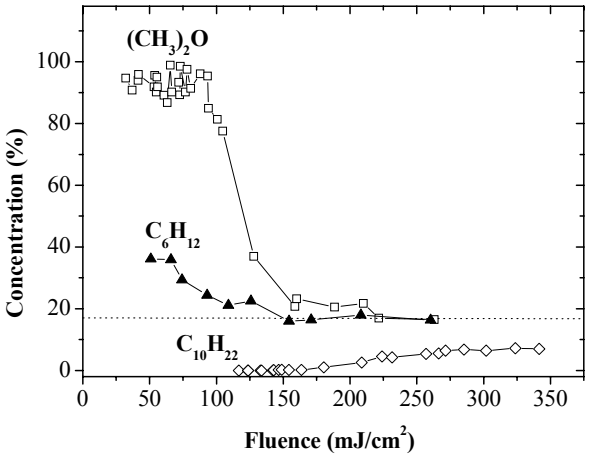

Fig. 4. Mass spectrometric measurements (λ=248 nm) of the concentration [i.e. $I_{dopant}/(I_{dopant} + I_{toluene})$] of $(CH_3)_2O$, C_6H_{12} and $C_{10}H_{22}$ dopants in the plume as a function of the laser fluence in the irradiation of the mixtures of these compounds with $C_6H_5CH_3$. The intensities are corrected for the different relative ionization efficiencies of the compounds in the mass spectrometer. The horizontal line indicates the initial concentration of dopants in the sample. The ablation thresholds for the corresponding systems are different due to different heat capacities and cohesive energies of the two systems, as a result of the dopant incorporation.

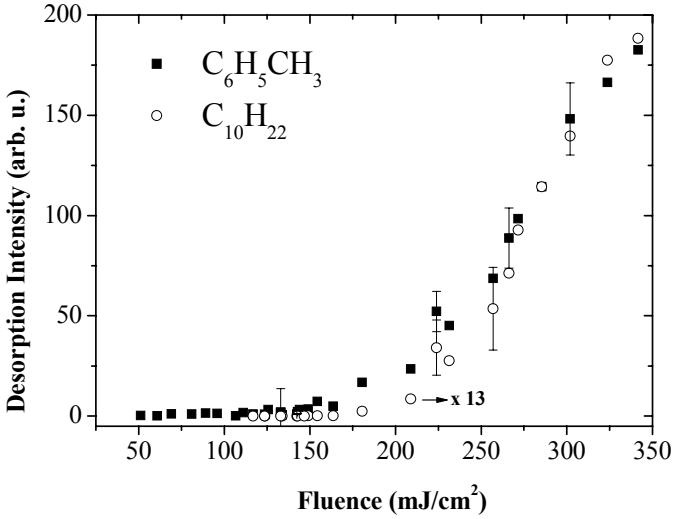

Fig. 5. Desorption intensities of $C_{10}H_{22}$ and of $C_6H_5CH_3$ in the irradiation of their mixture (1:5 molar ratio) at λ=248 nm.

These characteristics are not due to a change in the absorption process, since the absorptivity is measured to remain constant at least for laser fluences up to the ablation threshold. **Thus, the strikingly different ejection features at high laser fluences from those at low laser fluences unambiguously demonstrate the operation of different ejection mechanisms in the corresponding ranges. Accordingly, the ablation threshold represents a physically significant parameter.** The onset of the ejection of the strongly-bound to the matrix dopants constitutes a direct experimental criterion for establishing the laser ablation threshold of molecular solids.

According to the MD simulations [32], the onset of ablation is reflected by the ejection of material largely in the form of clusters. This criterion is different from the one established above in the experiments. However, further evidence indicates that they are closely correlated. Specifically,

MD simulations have been performed on some of the systems presented above [39]. Although the values adopted for some parameters differ from the experimental ones (due to computational limitations), there is overall very good agreement with the experimental results [39].

Most importantly, the simulations indicate that the strongly bound dopants are found exclusively within clusters of the matrix, whereas the weakly bound ones are ejected mainly as monomers. Clusters have been commonly observed in ablation studies of a wide range of materials. In the case of frozen substrates, cluster ejection is a particularly common observation in the irradiation of frozen aqueous solutions of salts (e.g. of $CeCl_3/H_2O$, $XMnO_4$ (X=Na, K)/ H_2O etc) [44]. Cluster observation has also been documented in the laser irradiation of a number of other cryogenic/ frozen compounds, though generally the cluster size distribution in these systems is not as extensive (broad) as in the case of frozen solutions of salts. We have discussed in detail elsewhere [45] the several factors that may be involved and determine cluster detection in laser ablation studies.

The important point, however, is that the clusters are ejected directly from the substrate and they are not mainly formed by secondary collisions in the plume (as usually suggested in most studies). Of course, depending on their internal energy and the number of collisions they undergo in the plume, a number of clusters may be disintegrated. Yet, in all cases, the MD simulations [32] find that in the initial stage, the strongly-bound-analytes/ dopants are ejected within clusters of the matrix/ solvent. This indication will be further justified within the "explosive boiling" model (Section 4b). Thus, the two criteria advanced by these experimental studies and the MD simulations appear, though still not proven experimentally, to be intimately interrelated.

2.1. Implications for MALDI, MAPLE

The results account for various observations in MALDI studies and have immediate implications for MAPLE. First, they account for the observation that the matrix desorbates are detected at fluences much lower than the biopolymers/ proteins [3]. In MALDI studies, the reason for this observation has been difficult to establish because ions are usually detected. Thus, the difference between the two detection limits has been plagued by arguments about the contribution of the ionization/ detection efficiency of the biopolymers [[46]-[47]]. However, here, this issue is altogether avoided, since neutral desorbates are detected. Clearly, our results show that there is a minimum threshold for ejection of the biopolymers in the gas phase: at lower fluences only the relatively volatile matrix/ solvent can desorb (because of the thermal nature of desorption), whereas ejection of the biopolymers, due to their high average binding to the aqueous solution [48], can be effected only in the ablative regime. Besides the mechanistic importance, this finding also shows the limitations in trying to obtain better films by reducing the employed fluences. It has been reasonably thought (both in MAPLE and MALDI studies) that deleterious chemical modifications/ fragmentation of the ejected biopolymers can be reduced by employing lower and lower laser fluences. Clearly, the improvement that can be attained is limited by the existence of a lower fluence limit for the ejection of the biopolymer.

The second important point concerns the influence of clustering on gas-phase desorbate intensity measurements. Since the interaction of the biopolymer with the matrix may be strong, the biopolymer may not get rid of its solvation shell through collisions in the plume. Clustering can significantly affect ionization, with species (within the clusters) with lower ionization potential being preferentially ionized [49]. As a result, the ion intensities recorded by electron impact or multiphoton ionization may not reflect accurately the relative concentrations of the neutral species in the plume. This factor accounts for the fact that the strongly bound dopant-to-matrix intensities ratio, as defined by mass spectrometry (Figure 4), appears to be lower than the film stoichiometry (these species have a higher ionization potential than $C_6H_5CH_3$). Thus, ejection of species within clusters may be of major analytical handicap. On the other hand, for deposition processes, it may be beneficial, as the incorporation of the biopolymers within clusters may ensure their "soft" landing on the target, as well as minimization of interaction between adsorbates that may lead to coagulation. However, it may imply that the deposit obtained is of lower chemical purity (which is likely of no importance if H_2O is the solvent [50], but may be a problem when other solvents are employed [51]).

Furthermore, the described studies clearly indicate the limitations/ caveats of Arrhenius-type analysis of ejection signals. In the present case, such analysis would indicate the same activation energy of ejection for the involatile species as for toluene. As demonstrated here, however, this value differs much from the binding energy determined by thermogravimetric measurements. The activation energies specified in the ablative regime do not relate to the binding energy of the specific molecules but, as shown in Section 4b, to the activation energy for "explosive boiling" (i.e., bubble nucleation energy).

A common argument is that ablation may just be defined by a high amount of material/ matrix being ejected. For matrices of a low cohesive energy, simple thermal desorption will result in a very high desorption signal (according to $e^{-\Delta E_{binding}/kT}$). Yet, this does not imply ejection of the incorporated biopolymers. The criteria for ensuring biopolymer ejection differ, as discussed in detail above.

3. Chemical processes and effects in the uv irradiation of cryogenic solids

It has often been argued that results on chlorinated (e.g. halocarbons-CH_xCl_y) solvents are inconsistent with the thermal model. For instance, for such solids the temperatures, as estimated on the basis of the absorption coefficient of the compounds, are too low at the ablation thresholds (at 248 nm) for any substantial thermal desorption/ evaporation [52]. Thus, a photochemical or a photomechanical mechanism has been implied, though these mechanisms were also indicated to fail to account for the observations. However, in these studies, a multipulse protocol was used. As shown below, for photochemically active compounds, multipulse protocols can result in significant complications.

More generally, the question arises about plausible chemical effects in the UV ablation of cryogenic solids. To this end, we give here a more general discussion of the chemical processes under intense laser irradiation conditions of cryogenic films. Studies have been performed in the UV (248 nm and 193 nm) irradiation of a number of systems such as CH_xCl_y (x=1-4), C_6H_{12}, C_6H_5Cl and H_2O. These compounds represent a wide range of absorptivities and different reactivities. Yet, in all cases, we have observed similar trends in the chemical processes induced upon UV irradiation of their condensed solids, so we review the general trends by giving selected examples.

Table 2 presents the (neutral) products detected *in the gas phase* (by quadrupole mass spectrometry) in the laser irradiation of cryogenic films/solids of the indicated compounds in the ablative regime [[41], [53]-[58]].

Table 2:

System	λ (nm)	Observed Products/Fragments[1, 2]	Refs
ClNO	193	Cl_2, NO, Cl	
ICl	532, 266	I, Cl, I_2, Cl_2	[59], [60]
Cl_2	355	Cl	[61]-[63]
C_6H_5Cl	248	(Cl)[3], C_6H_5, HCl, $C_{12}H_{10}$, C_6H_6 $C_6H_4Cl_2$, $C_{12}H_9Cl$, $C_{12}H_8Cl_2$	[56]
CH_3Cl	248	CH_3, CH_4, HCl, C_2H_6, C_2H_5Cl, $C_2H_4Cl_2$, (Cl)[3]	[54], [55]

[1] Besides the parent molecule.

[2] Radicals are generally difficult to be specified with electron-impact ionization and, thus, their presence cannot be ascertained. In the case of C_6H_5Cl,quantification of C_6H_6 is hampered by the contribution of the strong $C_6H_5^+$ peak deriving from the mass cracking of C_6H_5Cl.

[3] Cl detected only at high fluences.

Fig. 6a represents the intensity of the products observed in the gas-phase in the irradiation of neat C_6H_5Cl films (with a single laser pulse) as a function of F_{LASER}. In all cases, HCl is observed even from the lowest examined fluences ($\leq$ 5 mJ/cm^2 i.e. well-below the ablation threshold of the systems) from the very first pulse on freshly deposited films (Figure 6b). In contrast to HCl, most other products [e.g. in the irradiation of C_6H_5Cl the phenyl products $(C_6H_5)_2$, $C_6H_4Cl_2$, C_6H_5-C_6H_4Cl, $(C_6H_4Cl)_2$] for the first pulses on freshly deposited solids are detected in the gas phase only at fluences above the ablation threshold, whereas below the ablation threshold, they are detected only after extensive irradiation (when as shown below, signal induction becomes significant). It would appear that phenyl products are not formed at lower fluences. However, this is not the case, as examination by Thermal Desorption Spectroscopy (TDS) and High Resolution Electron Energy Loss Spectroscopy (HREELS) demonstrate [59] photolysis of C_6H_5Cl upon UV irradiation of multilayer films to be significant even at fluences < 1 mJ/cm^2. Furthermore, in the irradiation at fluences below the threshold, film transmission is found to decrease with successive laser pulses, thus indicating the accumulation in the film of biphenyl species, which are known to absorb much stronger than the parent compound at 248 nm [54]. Exactly similar observations have been made in the irradiation of chloroalkanes (CH_xCl_y) and C_6H_{12} at 248 nm. Thus, even at low fluences, well below the ablation threshold, all these products are formed, and the main or exclusive reason for failing to observe them in the gas phase relates to the fact that at these laser fluences, they cannot desorb thermally, because of their high binding energy to the matrix. Thus, relying exclusively on gas-phase diagnostics for assessing the photoinduced chemical processes and products can be misleading if examination is limited at low fluences, i.e., below the ablation threshold. If such a study is complemented by a parallel spectroscopic examination of the film, it will demonstrate a pronounced accumulation of species and extensive chemical modifications.

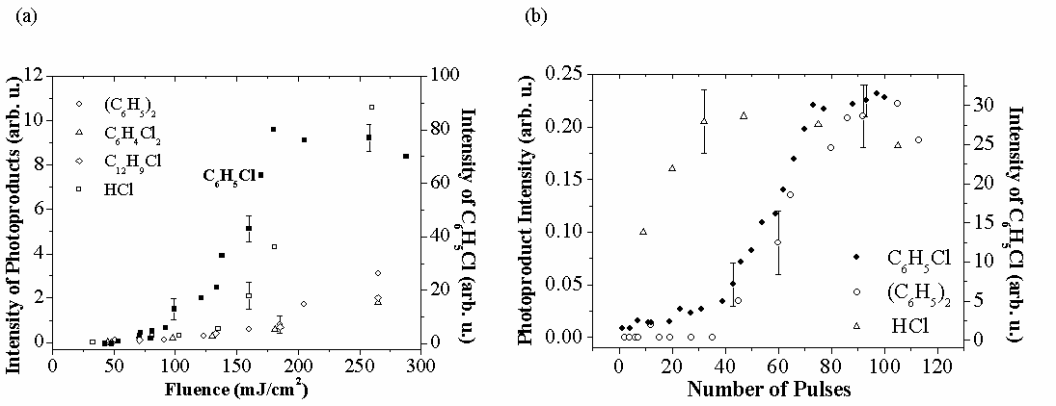

Fig. 6. (a) Products observed in the irradiation of condensed C_6H_5Cl solids at 248 nm as a function of the incident laser fluence (each signal is recorded in a single laser pulse from as-deposited solid). The right side axis corresponds to the intensity of the parent peak. (b) Pulse evolution of the ejection intensities of C_6H_5Cl, HCl and $(C_6H_5)_2$ in the irradiation of as-deposited films at 30 mJ/cm^2. The same pulse dependence as that for $(C_6H_5)_2$ is also observed for $C_6H_4Cl_2$ and $C_{12}H_9Cl$ (reprinted from Ref. [55] with permission).

For the halo-derivatives, the observed photochemistry is fully consistent with radical reactivity of the fragments produced upon UV photolysis of the compounds. For instance, in the case of C_6H_5Cl upon excitation with UV light, it dissociates exclusively by C-Cl bond scission to give phenyl radical and chlorine atom. Generally, for these compounds (C_6H_5Cl, CH_xCl_y etc.), thermal decomposition can be safely discounted because the attained temperatures (Section 5) are rather low, whereas the energies of the bonds involved (C-H, C-Cl) are quite high. Note that in this scheme, at least for 308 nm and 248 nm irradiation, Cl does not represent Cl detectable in the gas phase: for all examined halocarbons at these wavelengths, Cl is detected only at fluences well above the ablation threshold. This is understandable: Cl is so reactive that it reacts by H-atom-abstraction (if H-atom-containing groups are available) that any Cl produced in the film by

photolysis will react before ejection. Free Cl is only observed at high fluences and must be formed by secondary photolysis of ejecta in the rarefied part of the plume, consistent with the fact that the Cl time-of-flight differs significantly from that of the parent compounds both in width and peak arrival time, and the E_{TRANS} is comparable to that determined in the gas- phase photolysis of the compounds, (thereby suggesting that it has undergone very few collisions). On the other hand, at 193 nm for all chlorinated compounds [[41], [54]-[55]] a high signal for free Cl is generally observed and its time-of-flight characteristics are more complex, indicating that at 193 nm, even Cl formed in the film may be ejected before reaction (plausibly because of higher kinetic translational energy acquired upon photolysis or because of faster plume ejection at 193 nm).

Note that product formation can be significant even in the case of "seemingly" photoinert compounds such as C_6H_{12} at 248 nm. C_6H_{12} at moderate laser fluences at 248 nm undergoes two-photon excitation/ ionization, with the ions reacting subsequently to form a variety of UV-absorbing products. Note also that usually deleterious chemical modifications are generally thought to relate to plasma effects: evidently this is not the case.

The most important, however, implication is that for irradiation at fluences below the ablation threshold, the extensive accumulation of products in the film (due to their inefficient thermal desorption) may result in a significant change of the absorptivity (Figure 7a). This effect is most pronounced in the irradiation of solids of weakly absorbing compounds, such as of halocarbons (CH_xCl_y) and C_6H_{12} at 248 nm and 308 nm, but is also observed even in the irradiation of moderately absorbing ones (e.g. C_6H_5Cl at 248 nm) (in the UV). As a result of the gradual accumulation of highly absorbing products and the consequent change in laser energy absorption, ejection efficiency at fluences below the ablation threshold increases with successive laser pulses, i.e. signal induction (incubation) occurs (Figure 7b). The same dependence of the signal on successive laser pulses is observed by a wide angle (open) ionization gauge placed close to the irradiated solids, thus this change in the mass spectroscopic signal is not due to changes in the angular distributions of the ejecta. In the case of polymers, induction is a well-known effect [[1], [2], [5]], especially for irradiation at weakly absorbed wavelengths (e.g. PMMA at 248 nm) and the physical basis (mechanism) appears to be the same as for cryogenic solids.

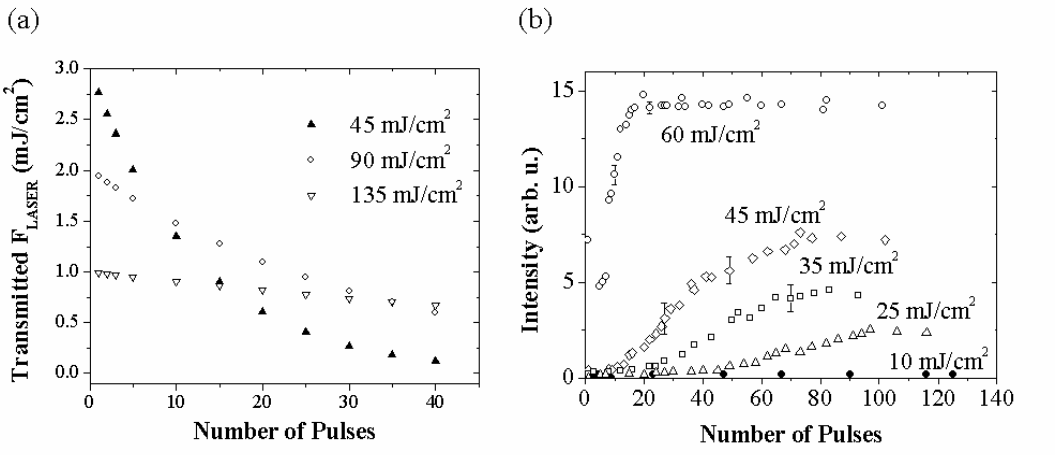

Fig. 7. (a) The transmittance of a C_6H_5Cl film at 248 nm upon irradiation with successive laser pulses at 248 nm. (b) Induction effect for C_6H_5Cl at 248 nm at various fluences (reprinted from ref. [55] with permission).

Clearly, in systems that induction is important, particular care must be paid when interpreting the results from multipulse laser irradiation experiments. First, the average "etching/ desorption yield" from multiple pulse experiment can differ significantly from the pulse-to-pulse value. In addition, it can be misleading: at moderate fluences, for the first few pulses, the process is in the sub-ablative regime, in which case the strongly-bound-to-the-matrix dopant is not ejected; but, after a sufficient number of pulses, ablation sets in and the biopolymer will be efficiently ejected in the gas phase. However, because of the parallel accumulation of other products in the

film, the possibility for chemical degradation of the biopolymer is higher than in the ablative regime. Most importantly, estimating the laser-induced temperatures on the basis of the absorption coefficient of the parent compound is erroneous. The discussion of mechanisms must be accordingly reconsidered (e.g., the attained temperatures are much higher than estimated, at variance with the arguments of Ref. [52]).

4. Mechanisms of UV ablation

4.a. Overview of mechanisms

Excluding the simple thermal evaporation/ desorption scheme, three, at least, different mechanisms have been considered in the literature for laser-induced material ejection, namely photochemical, photomechanical and phase explosion [[1], [2]]. All three can account for massive, unselective material ejection, but they differ considerably in their nature.

According to the photochemical mechanism, material ejection is due to the expulsion exerted by gaseous products and fragments produced by the photolysis of the parent molecule. This mechanism has been advanced [[65], [66]] in a number of cases e.g. by Masuhara and coworkers for the UV ablation (at 248 nm) of aromatic compounds *in liquid state* (under ambient conditions). In the case of $C_6H_5CH_3$, the photochemical mechanism can be rejected on the basis of a number of experimental observations [67]. For instance, in the irradiation of $C_6H_5CH_3$ films, no products are detected by mass spectrometry upon UV laser irradiation. On the other hand, a photochemical mechanism may be contributing in the ablation of photolabile compounds. Indeed, MD simulations reported recently [68] on our previous work on C_6H_5Cl indicate that the ablation threshold is lower than if no reactions take place.

A spallation/ photomechanical mechanism has sometimes been considered. A detailed assessment of its contribution in the case of glycerol matrices has been given in [69]. Generally, however, its contribution for typical excimer laser pulses and relatively strongly absorbing systems can be considered to be rather moderate. In the present case, it can be rejected because of the weak stress confinement: $\tau = \frac{1}{\alpha c} \cong \frac{1}{3700\,cm^{-1} 1500\,cm/\sec} < \tau_{pulse}$~30 ns, where α is the absorption coefficient and c is the speed of sound in the material.

For the purposes of this review, we focus particularly on explosive boiling, because (1) according to our studies, at least for photoinert, moderately strongly absorbing systems, it appears to be dominant in nanosecond laser ablation (2) its implications for MALDI/ MAPLE have not been discussed in detail, so that various difficulties in accepting it are not well founded and (3) it directly relates to fundamental issues in nanoscience/technology.

4b. Explosive boiling

Liquids heated above the temperature corresponding to the equilibrium external pressure are thermodynamically metastable (Fig. 8), since their chemical potential μ_L is higher than that of the vapor μ_V [[33], [70], [71]]. However, the transformation (boiling) requires bubble formation, which is limited by the work necessary for the formation of a new interface within the liquid (i.e., the surface tension σ) [70]. The free energy for bubble formation is:

$$\Delta G = 4\pi R^2 \sigma - \frac{4}{3}\pi R^3 (P_V - P_L) + \frac{4}{3}\pi R^3 \frac{P_V}{k_B T}(\mu_V - \mu_L) \quad (1)$$

where R is the bubble radius, σ the surface tension, k_B the Boltzmann constant, T the saturation temperature of liquid and P_V, P_L are respectively the pressure inside the bubble and the ambient pressure of the liquid. In the above equation, the first term represents the energy necessary for the liquid-vapor interface formation, the second one the work directed against the pressure forces and the third one the "driving force" of bubble formation. For small R, the surface term dominates and so $\Delta G>0$; only for sufficiently large R, $\Delta G<0$ as necessary to lead to bubble growth. The radius for this change is specified by the condition of "mechanical" equilibrium of the bubble

$\left(P_V - P_L = \frac{2\sigma}{R}\right)$ and of "thermodynamic" equilibrium $\left(\mu_L(P_L) = \mu_V(P_{sat})\right)$ [where P_{sat} is the saturation pressure of the liquid phase]. This radius is donated as the "critical" radius and in this case $\Delta G_{cr} = \frac{16\pi\sigma^3}{3(P_V - P_L)^2}$. Thus, the rate at which homogeneous bubbles of critical size are generated (J_{cr}) is given by:

$$J_{cr} = J_0 \exp\left(-\Delta G_{cr}/k_B T\right) = J_0 \exp\left(-\frac{16\pi\sigma^3}{3k_B T(P_V - P_L)^2}\right) \quad (2)$$

where $J_0 = N_L\left(\frac{3\sigma}{\pi m}\right)^{1/2}$ (N_L is the number of liquid molecules per unit volume and m is the molar mass). Because in (2) both σ and (P_V - P_L) factors depend sensitively on temperature, critical bubble formation depends crucially on the maximum attained film temperature and its temporal evolution.

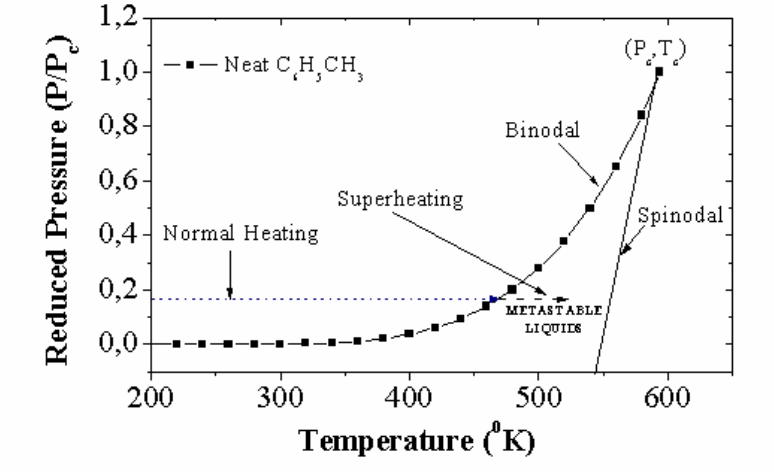

Fig. 8. The binodal and spinodal curves and the region of metastability for toluene. C is the critical point, and T_C=593 ^{0}K and P_C=41 bar are respectively the temperature and the pressure of the compound at the critical point.

The surface film temperature drops rapidly after the end of the laser pulse as a result of evaporative cooling (Fig. 9). For low overheating, the reduction in the free energy upon phase change is insufficient to compensate for the surface tension limitation and, thus, bubble growth eventually halts (~ 100 ns). However, with increasing fluences/ temperatures, due to the sharp decrease of σ and the increase of $(P_V\text{-}P_L)^2$ factors, J increases sharply. At a sufficient degree of superheating, the number of interconnected bubbles and high pressure exerted by them result in the violent (supersonic beam-like) material ejection. Because J increases sharply exponentially, the onset for material ejection exhibits a "threshold-like" behavior. In fact, thermodynamic analysis [33], as well as the MD simulations [32] associate the threshold with the limit (maximum T) that can be effected before a liquid becomes so unstable that "spontaneously" (i.e., without the requirement of an energy barrier to be overcome) decomposes into a mixture of liquid/ gas. This limit, spinodal limit, is specified [[70], [72]] by the criteria $\left(\frac{\partial P}{\partial V}\right)_T = 0$ and $\left(\frac{\partial S}{\partial T}\right)_P = 0$ (stability criteria) and occurs at ~ $0.8T_c$, where T_c is the critical point of the compound.

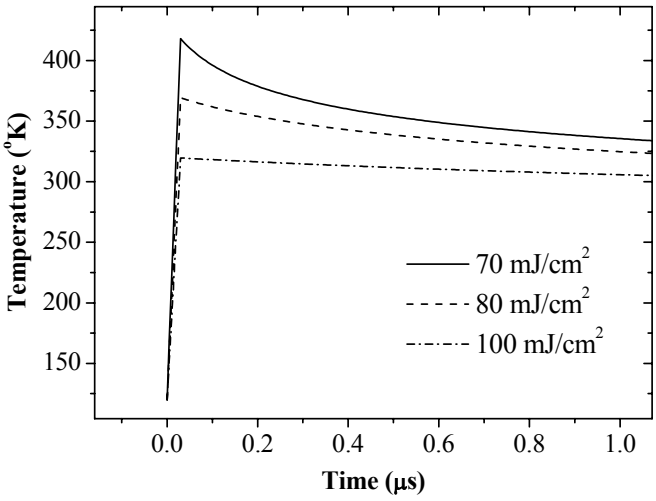

Fig. 9. The surface film temperature as a function of time for the indicated laser fluences.

The suggestion of explosive boiling can account consistently for several features of laser ablation at least of photoinert systems (with ns laser pulses):

It accounts for material ejection largely in the form of clusters/ droplets as suggested by the MD simulations. Indeed, even for heating of a system up to the spinodal limit (T_{sp}) the required heat $c_p(T_{sp}-T_0)$ (per unit mass) is lower than the evaporation energy (per unit mass), i.e., the available heat is not sufficient for the complete evaporation to monomers. A detailed thermodynamic justification is given by Debenedetti [70] and the reader is referred therein. The important point to underline here is that due to material ejection largely in the form of liquid droplets, the "activation energy" will be lower than expected on the basis of the sublimation/ evaporation energy of the compound.

Explosive boiling can provide a solid justification for the common observation in MAPLE studies that better results are obtained for "volatile" solvents. Specifically, the minimum energy (per unit volume or mass) for explosive boiling relates to the cohesive energy of the substrate (i.e., the intermolecular binding energy), decreasing with decreasing cohesive energy [[39], [72]]. This is clearly illustrated by the comparison of the critical points T_C for a series of hydrocarbons of increasing molecular length (thus, increasing pairwise additive interactions) (nominally, explosive boiling occurs at ~0.8 T_C). Alternatively, this dependence can be rationalized within the framework of conventional nucleation theory by the fact that a higher cohesive energy of the system results in an increase of the surface tension and a decrease of P_V, thus higher temperatures (T) are required for significant bubble growth (Eq. 2). Thus, for "volatile" solvents, i.e. solvents of low cohesive energy, explosive boiling can be effected at relatively low fluences (temperatures), thus ensuring minimal thermal or photochemical influence on the biopolymers. Based on this, we suggest that fluoro-compounds (characterized by low cohesive energy) would be excellent solvents for MAPLE, if of course the polymer is soluble in them.

The assumption of explosive boiling also provides a rational for the ejection of the "involatile" species exclusively within clusters of the matrix/ solvent. Adopting the kinetic Kagan-Domler description [[70], [73]] the rate of vaporization into the bubbles can be approximated by $\frac{A}{(2\pi m k_B T)^{1/2}}\left[P_V(T) - P_L\right]$, where A is correlated with the fraction of dopant on the bubble "surface", $P_V(T)$ is the vapor pressure of the compound at the (laser-induced) temperature T_V, P_L is the ambient pressure on the liquid and m is the mass of the molecule. For mixtures, an additional factor is usually included for accounting for replenishment of the molecules vaporized into the bubble by diffusion from the bulk [70], but in the case of MALDI and MAPLE, this factor can be neglected. Therefore, the relative desorption rates of the two components (dopant, matrix) into the

bubbles is specified by $e^{-E_{dopant}} / e^{-E_{matrix}}$, where E represents the binding energy of the component in the condensed phase. Thus, in the case of "involatile" dopant (high $E_{binding}$), the growing bubbles are exclusively composed of $C_6H_5CH_3$ vapor, and explains the finding of the MD simulations that the strongly bound dopants are ejected exclusively within droplets of the matrix. The implication for MAPLE and MALDI is that, thermodynamically, it is much more "facile" to break the weak bonds between the outer solvent layer of the cluster surrounding the biopolymer than breaking the large number of the rather strong (hydrogen type) bonds between the biopolymer and the solvent. Thus, explosive boiling provides a simple and physically acceptable picture of how strongly bound biopolymers are ejected at relatively low temperatures.

5. Phase transformations and bubble formation

A fundamental implication of the "explosive boiling" mechanism is that upon irradiation even at fluences below the ablation threshold, the solid melts. However, no direct experimental evidence of a solid-to-liquid phase transformation has been obtained so far, except for indirect observations via studies of the translational distributions of the desorbates [44] and post-irradiation optical examination of the morphology of irradiated areas. The second fundamental feature entailed in explosive boiling is the formation of bubbles within the (superheated) liquid.

Considering first the issue of melting, calculations indicate that for neat $C_6H_5CH_3$, the matrix attains sufficient (at the surface) temperature to melt (T_m ~ 178 ^{0}K) at F_{LASER} ~ 30 mJ/cm^2, i.e. well below the ablation threshold (~ 100 mJ/cm^2). Hence, the increase in the desorption intensity of neat $C_6H_5CH_3$ observed at ~ 45 mJ/cm^2 (Figure 3, inset) is ascribed to the melting of the film. Melting is directly demonstrated by the pulse dependence of the intensity of "volatile" dopants (e.g. $(CH_3)_2O$). For irradiation at fluences < 50 mJ/cm^2, the dopant signal is found to decrease with successive laser pulses. The total signal over ~ 50-100 pulses indicates that only dopant from the upper (surface) layer (~ 10 nm) of the film desorbs. In contrast, in the 50-100 mJ/cm^2 fluence range, though the dopant signal per pulse is much higher, and the total signal over the first ~ 25-50 pulses corresponds to desorption of the dopant from ~ 100 nm depth. Diffusion of the dopant from such depths shows that the film viscosity is in the ~ 10^3-10^{-3} Pa·s range, which in fact corresponds to the viscosity of liquid toluene (for T=210-350 K) [75]. In contrast, the viscosity of (frozen) $C_6H_5CH_3$ at ~100 K is ~10^{12} Pa·s [75].

At F_{LASER} ρ 40-50 mJ/cm^2, the melt, under the effective zero external pressure, represents a metastable liquid that may undergo explosive boiling [[72]-[74], [76]]. Therefore, bubble nucleation/ formation is expected. Bubble formation/ growth may be detected by optical techniques, as for example demonstrated in the superheating of liquids adjacent to absorbing surfaces [[77]-[81]]. However, molecular substrates are generally amorphous/ powdery (thus, highly optically scattering), thereby limiting the potential of optical techniques in these substrates. In our studies, we have overcome this problem by exploiting the fact that upon vapor condensation at temperatures □120 ^{0}K, toluene forms a glass of high optical quality (in the VIS) [82]. The processes that are induced to the glass upon UV (248 nm) irradiation are monitored via imaging and temporally resolved monitoring of the transmission/ reflection of a probe beam (HeNe or diode laser) [83]. Briefly, a sharp characteristic decrease of the intensity of the transmitted/ reflected probe beam is observed at ~60-200 ns after the UV laser pulse (Figure 10). The decrease gets more pronounced with increasing laser fluence, reaching maximum close to the ablation threshold. At fluences above the ablation threshold (100 mJ/cm^2), this peak is followed by a broad decrease (~ 10s μs) of the transmitted/ reflected probe beam. This second broad decrease is evidently due to the scattering of the probe beam by the ejected plume. On the other hand, the sharp decrease at ~ 100 ns shows close similarities (in time and shape/ time-decay) with the optical transients that have been observed for bubble growth in the case of superheating of liquids adjacent to laser heated surfaces [80]. Indeed, in the present case, a Rayleigh-Gans [84] type analysis of the signals indicates the size of scatterers to be in the 60-100 nm range, consistent with gaseous bubbles.

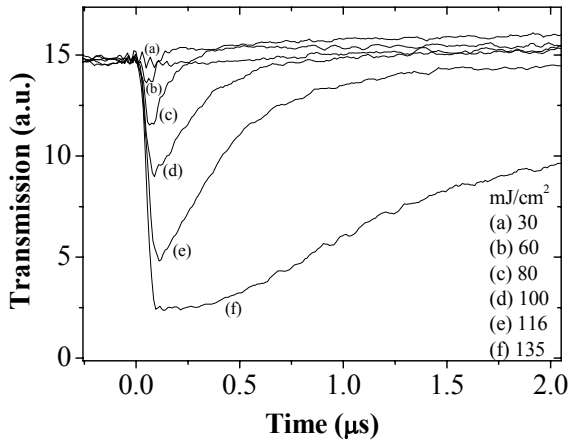

Fig. 10. Time-resolved transmission at λ=633 nm, recorded upon irradiation of condensed $C_6H_5CH_3$ films with one UV pulse (λ=248 nm) at the indicated fluences.

In fact, besides bubble formation, we have observed a number of structural transformations for these simple organic substrates/ glasses upon laser irradiation (such as glass devitrification at low fluences (15-30 mJ/cm^2). Besides their importance for the mechanistic elucidation of laser-induced desorption/ ablation processes, their observation is important in relationship with the elucidation of dynamics of molecular glasses/amorphous solids, a topic of intense current interest in physical chemistry.

Relevant to structural aspects, it is important to note that the targets/substrates obtained upon cooling are usually highly polycrystalline. Therefore, even in the absence of any chemical modifications, optical properties may differ considerably from those determined from measurements on liquid samples. Furthermore, the exact structure depends on the rate of cooling. Different cooling rates result in different polycrystalline structures, with somewhat different coordination number of the molecules and, thus, of their intermolecular binding. Because the desorption intensity depends exponentially on the binding energy, these changes can result in significant variation of the desorption/ejection yields. For instance, in the case of vapor-deposited toluene (at ~100 K), upon annealing the film, the signals in Fig. 3 decrease by nearly a factor of 2. It is interesting to note that in MALDI [[85]-[87]], a pronounced dependence of the biopolymer (ion) signal on the substrate structure, i.e., degree of crystallinity is observed. In fact, this high sensitivity of ejection to the matrix structure (i.e. degree of polycrystallinity) has been one of the major problems in the development and optimization of MALDI. Likely, this dependence on structure can account for variations of results that are sometimes noted in MAPLE studies.

Furthermore, irradiation of the film further affects its structural condition. Thus, for compounds in which induction does not occur, at relatively low fluences, previous irradiation results in laser annealing of the as-frozen samples, and often the desorption signal decreases somewhat with successive laser pulses (i.e. even in the absence of formation of a crater). Of course, signal dependence on solid structure is particularly high in the ablative regime, where the formation of a crater affects also the angular distribution of ejecta, etc.

6. Bubble dynamics and nanoscience/ technology

Of course, further studies are required for establishing in detail how in MAPLE and MALDI explosive boiling affects biopolymer ejection. Nevertheless, it must be realized that explosive boiling is a much more general/ubiquitous phenomenon, of fundamental scientific interest, and also of direct relevance to nanoscience/technology.

Despite all studies for over 100 years, especially the primary steps in bubble nucleation/ formation remain unclear (ambiguous). There are many instances in liquids, under ambient atmosphere, at which pronounced differences are found between the predictions of the classical nucleation theory and experimental results. The best known and most extensively studied example concerns cavitation (the process of bubble formation by reducing the pressure on the liquid), for which inception occurs at acoustic amplitudes far below the theoretically predicted tensile pressure (e.g. the experimental tensile strength of H_2O is almost order of magnitude below the predicted value [[70], [72], [88]]). Discrepancies have also been noted in the explosive boiling processes in the laser-irradiation of liquids and of liquids adjacent to laser-heated surfaces. However, in liquids, exclusion of dissolved gases (that may act as heterogeneous nuclei) cannot be prevented. Thus, any deviations between theory and experiment have been largely attributed to the hypothesis that long-lived cavitation nuclei, such as ultramicroscopic bubbles are present in liquids.

The above hypothesis appears to account for the observed deviations but, in fact, it introduces an even more fundamental problem. Bubbles with a radius smaller than R_{cr} are thermodynamically unstable (Section 4b) and should dissolve and vanish quickly. For resolving this difficulty, Frenkel [89] has resolved to the distinction between heterophases and homophases, but the physical basis for this delineation is unclear. Alternatively and equally questionably, stabilization of (nano) bubbles has been ascribed to the influence of such factors as cosmic radiation [90], formation of clusters of organic or ionic molecules [[91], [92]] and van der Waals stabilization [93]. In addition, bubble nucleation/ growth exhibits a quite complex behavior, which cannot be accounted by classical models. For highly purified and degassed water, a significant decrease of the cavitation threshold due to neutron irradiation has been observed [94], with the threshold slowly returning to the initial level upon removal of the source of radiation (kind of a memory effect). A "memory" effect has also been demonstrated by Leiderer and Grigoropoulos [79] on μs-ms time scale in the explosive boiling of liquids adjacent to solid (absorbing) surfaces heated by nanosecond pulses.

There is increasing understanding that the above discrepancies between theory and experiment are not only due to experimental limitations, but rather to our limited understanding and specification of parameters, e.g. of the surface tension, on nanometer scale. A common approach is to introduce the variation of the surface tension with curvature (Tolman's length) [95]. The problem is being vigorously attacked by simulations on the nanometer scale. It has already led to major new concepts concerning cavity formation within a liquid, hydrophobicity [[96], [97]] etc.

Besides the fundamental scientific interest, the above questions are also of direct relevance to nanoscience and nanotechnology. The existence of nanobubbles can be a serious problem in the examination of surfaces by in situ atomic force microscopy (AFM) and other scanning microscopies. Nanobubbles have been detected to form spontaneously when gold surfaces are immersed in pure water [98], but they are probably a general phenomenon at liquid-solid interfaces. Their formation can result in undesirable effects, such as enhanced noise and even artefacts in the microscopic imaging (solutions). Formation of nanobubbles is also common in the laser irradiation of materials. Laser-based structuring techniques generally result in some degree of heating. Thus, when using laser-based techniques for nanostructure fabrication, within liquids bubble formation may compromise the focusing of the beam and the final resolution of the structures produced by techniques such as femtosecond-based polymerization approaches [99]. On the other hand, nanobubble formation may be used to advantage. For instance, recently, bubble formation has been exploited for the directional transport of objects in microfluidics. Typically, actuation forces exploited to transport small objects in channels rely on applied pressure differences, capillary forces, electrophoresis or Marangoni forces [100]. By comparison with these approaches, microbubbles on a substrate can induce well controlled fluid motion on very small scales [101]. Furthermore, appropriate combinations ("doublets") of bubbles and microparticles provide for the controlled breaking of the symmetry of the motion. In other work, the rapid expansion of vapor bubbles has been exploited to switch valves in microdevices [102]. Bubbles have also been exploited for blocking transiently the path of a light beam, thus creating an optical switch [103]. Microbubble formation near cells can also result in localized shear forces sufficient to open pores in cellular membranes, thus enabling drug delivery or gene transfection [104].

Despite all this importance, the study of bubble nucleation and growth in liquids is subject to major limitations, due to the presence of dissolved ambient gases. In addition, the fleeting

existence of bubbles in liquids makes their study quite difficult. Generally, the time scale for most acoustic studies has been limited to microseconds due to the instability of the transducers to generate shorter acoustic pulses of sufficient intensities to cause cavitation. On the other hand, the use of cryogenic films (under high vacuum) offers the crucial advantage that the presence of dissolved gases or of impurities that may act as heterogeneous nuclei can be strictly excluded. Furthermore, because of the relatively rapid cooling (cooling on $1/a^2 D_{th}$ ~ 10-50 μs, where α is the absorption coefficient and D_{th} the heat diffusion constant) and subsequent solidification, bubble structures may be "arrested" and thus studied in detail. In addition, they can be monitored in time, thus being able to establish the factors crucial for elucidating their dynamics when still in their "infancy". It is clear that bubble formation in cryogenic films can provide new insights, as necessary for exploiting and manipulating bubbles at the nano level.

Indeed in our studies, we have noticed various discrepancies in the quantitative analysis of the dynamics of superheated liquids on ns time scale. Theoretical considerations generally associate ablation with spinodal decomposition, attained at temperatures ~$0.8T_c$, (~ 470 ^{0}K for toluene, where T_c is the critical temperature). However, we have noted in our experiments [67] that the estimated surface temperatures are somewhat lower e.g., for neat $C_6H_5CH_3$, the temperature at threshold is estimated to be ~ 350-380 ^{0}K. This value is certainly well above the melting point of toluene, but not quite as high as expected from the model. Very recently, Perez et al [105], on the basis of molecular dynamics have also indicated shortcomings of the accepted view of explosive boiling [33]. At any rate, the important point is that though the general theory [[72]-[74]] predicts ablation to occur at the spinodal limit, in practice, its onset is initiated at lower temperatures. This means that thermal degradation effects are considerably less than may be expected.

7. Conclusions

Significant information about MAPLE can be obtained from studies on cryogenic solids, where the mechanisms and processes of laser-induced material ejection have been addressed in detail, free from the complications encountered when using frozen polymer samples.

It was shown that biopolymers can be ejected in the gas phase only upon laser irradiation at fluences above the ablation threshold. At lower fluences, a thermal vaporization process operates, which can be responsible for the desorption of the solvent, but not of the polymer. Given this separation, quantitative analysis of the rates of biopolymer/ matrix activation energies of desorption can be quite misleading.

For photoinert compounds, explosive-boiling type process is shown to dominate. Several implications of explosive boiling mechanism have been examined in detail. It was shown that explosive boiling can account for most observations in the laser-material ejection (in cryogenic solids, MAPLE and MALDI) in a physically direct way. The important point is that biopolymers are not simply evaporated or ejected via collisions with the desorbing molecules to the same velocity. These ideas can result in several pitfalls, even if overall the working knowledge has empirically established the important parameters.

Typical chemical processes in the irradiation of various films have been presented. These provide better clue about the solvents that may be useful in extending the potential of MAPLE to other biochemical systems.

We have not discussed in this review the possibility of MAPLE with femtosecond pulses, since we are not aware of any reported studies. Furthermore, only preliminary studies on the ablation of cryogenic films with fs pulses have been reported. These studies indicate the high potential of femtosecond laser technology for film deposition, but in parallel they indicate that mechanisms and characteristics of material ejection differ substantially from the ones specified (described) above for nanosecond laser-induced material ejection.

Acknowledgements

We thank the UltraViolet Laser Facility operating at FORTH under the Improving Human Potential (IHP)-Access to Research Infra-structures program (contract no. HPRI-CT-1999-00074).

We thank several previous coworkers, in particular A. Koubenakis, J. Labrakis, A. Michalakou, K. Stamataki, as well as collaboration with B. J. Garrison group (Penn State University).

References

[1] J. C. Miller, Laser Ablation, Principles and Applications, vol. 28, Springer Ser. Mater. Sci., Berlin (1994).
[2] D. Bäuerle, Laser Processing and Chemistry, Springer-Verlag: Berlin (2000).
[3] K. Dreisewerd, Chem. Rev. **103**, 395 (2003).
[4] F. Hillenkamp, M. Karas, Int. J. Mass Spectrom. **200**, 71 (2000).
[5] J. C. Miller, R. F. Jr. Hanglund, Laser Ablation and Desorption, Experimental Methods in the Physical Sciences, vol. 30; Academic Press: San Diego, CA (1998).
[6] M. Karas, F. Hillenkamp, Anal. Chem. **60**, 2299 (1988).
[7] A. Vogel, V. Venugopalan, Chem. Rev. **103**, 577 (2003).
[8] S. Georgiou, V. Zafiropulos, D. Anglos, C. Balas, V. Tornari, C. Fotakis, Appl. Surf. Sci. **127-129**, 738 (1998).
[9] D. B. Chrisey, G. K. Hubler, Pulsed Laser Deposition of thin films, Wiley-Interscience: New York (1994).
[10] A. Klini, A. Manousaki, D. Anglos, C. Fotakis, J. Appl. Phys. **98**, 123301 (2005).
[11] D. M. Bubb, R. A. McGill, J. S. Horwitz, J. M. Fitz-Gerard, E. J. Houser, R. M. Stroud, P. W. Wu, B. R. Ringeisen, A. Piqué, D. B. Chrisey, J. Appl. Phys. **89**, 5739 (2001).
[12] D. M. Bubb, J. S. Horwitz, J. H. Callahan, R. A. McGill, E. J. Houser, D. B. Chrisey, M. R. Papantonakis, R. F. Hanglund Jr., M. C. Galicia, A. Vertes, J. Vac. Sci. Technol. A **19**, 2698 (2001).
[13] R. Cristescu, I. Stamatin, D. E. Mihaiescu, C. Ghica, M. Albulescu, I. N. Mihailescu, D. B. Chrisey, Thin Solid Films **453**, 262 (2004).
[14] G. Socol, P. Torricelli, B. Bracci, M. Iliescu, F. Miroiu, A. Bigi, J. Werckmann, I. N. Mihailescu, Biomaterials **25**, 2539 (2004).
[15] M. L. Popescu, R. M. Piticescu, S. Petrescu, L. Zdrentu, I. Mihailescu, G. Socol, W. Lojkowski, Rev. Adv. Mat. Sci. **8**, 164 (2004).
[16] A. Piqué, R. A. McGill, D. B. Chrisey, D. Leonhardt, T. E. Mslna, B. J. Spargo, J. H. Callahan, R. W. Vachet, R. Chung, M. A. Bucaro, Thin Solid Films **355-356**, 536 (1999).
[17] B. Toftmann, K. Rodrigo, J. Schou, P. Roman, Appl. Surf. Sci. **247**, 211 (2005).
[18] K. Rodrigo, B. Toftman, J. Schou, R. Pedrys, J. Low Temp. Phys. **139**, 683 (2005).
[19] D. M. Bubb, S. M. O'Malley, C. Antonacci, D. Simonson, R. A. McGill, J. Appl. Phys. **95**, 2175 (2004).
[20] K. Tanaka, H. Waki, Y. Ido, S. Akita, Y. Yoshida, T. Yoshida, Rapid Commun. Mass Spectrom. **2**, 151 (1988).
[21] D. B. Chrisey, A. Piqué, R. A. McGill, J. S. Horwitz, B. R. Ringeisen, D. M. Bubb, P. K. Wu, Chem. Rev. **103**, 553 (2003) and references therein.
[22] P. K. Wu, B. R. Ringeisen, D. B. Krizman, C. G. Frondoza, M. Brooks, D. M. Bubb, R. C. Y. Auyeung, A. Piqué, B. Spargo, R. A. McGill, D. B. Chrisey, Rev. Sci. Instrum. **74**, 2546 (2003).
[23] R. Cristescu, G. Dorcioman, C. Ristoscu, E. Axente, S. Grigorescu, A. Moldovan, I. N. Mihailescu, T. Kocourek, M. Jelinek, M. Albulescu, T. Buruiana, D. Mihaiescu, I. Stamatin, D. B. Chrisey, Appl. Surf. Sci. **252**, 4647 (2006).
[24] A. Doraiswamy, R. J. Narayan, R. Cristescu, I. N. Mihailescu, D. B. Chrisey, Mat. Sci. Eng. C **27**, 409 (2007).
[25] R. Cristescu, T. Kocourek, A. Moldovan, L. Stamatin, D. Mihaiescu, M. Jelinek, I. Stamatin, I. N. Mihailescu, D. B. Chrisey, Appl. Surf. Sci. **252**, 4652 (2006).
[26] R. Cristescu, T. Patz, R. J. Narayan, N. Menegazzo, B. Mizaikoff, D. E. Mihaiescu, P. B. Messersmith, I. Stamatin, I. N. Mihailescu, D. B. Chrisey, Appl. Surf. Sci. **247**, 217 (2005).
[27] R. Cristescu, D. Mihaiescu, G. Socol, I. Stamatin, I. N. Mihailescu, D. B. Chrisey, App. Phys. A **79**, 1023 (2004).

[28] T. M. Patz, A. Doraiswamy, R. J. Narayan, W. He, Y. Zhong, R. Bellamkonda, R. Modi, D. B. Chrisey, J. Biom. Mat. Res. B-Appl. Biomat. **78B**, 124 (2006).
[29] A. Doraiswamy, R. J. Narayan, T. Lippert, L. Urech, A. Wokaun, M. Nagel, B. Hopp, M. Dinescu, R. Modi, R. C. Y. Auyeung, D. B. Chrisey, Appl. Surf. Sci. **252**, 4743 (2006).
[30] I. Zergioti, A. Karaiskou, D. G. Papazoglou, C. Fotakis, M. Kapsetaki, D. Kafetzopoulos, Appl. Phys. Lett. **86**, 163902 (2005).
[31] D. Young, R. C. Y. Auyeung, A. Piqué, D. B. Chrisey, D. Dlott, Appl. Phys. Lett. **78**, 3169 (2001)
[32] [(a)] L. V. Zhigilei, P. B. S. Kodali, B. J. Garrison, J. Phys. Chem. B **101**, 2028 (1997).
[(b)] L.V. Zhigilei, E. Leveugle, B. J. Garrison, Y. G. Yingling, M. I. Zeifman, Chem. Rev. **103**, 321 (2003).
[(c)] L. V. Zhigilei, B. J. Garrison, J. Appl. Phys. **88**, 1281 (2000).
[33] R. Kelly, A. Miotello, Phys. Rev. E **60**, 2616 (1999) and references therein.
[34] S. Georgiou, E. Mastoraki, E. Raptakis, Z. Xenidi, Laser Chem. **13**, 113 (1993).
[35] K. Dreisewerd, M. Schürenberg, M. Karas, F. Hillenkamp, Int. J. Mass Spectrom. Ion Processes **141**, 127 (1995).
[36] [(a)] C. Focsa, C. Mihesan, M. Ziskind, B. Chazallon, E. Therssen, P. Desgroux, J. L. Destombes, J. Phys. Cond. Matt. **18**, S1357 (2006).
[(b)] C. Mihesan, N. Lebrun, M. Ziskind, B. Chazallon, C. Focsa, J. L. Destombes, Surf. Sci. **566**, 650 (2004).
[37] K. Domen, T. J. Chuang, Phys. Rev. Lett. **59**, 1484 (1987).
[38] A. Koubenakis, T. Elimioti, S. Georgiou, Appl. Phys. A **69**, S637 (1999).
[39] Y. G. Yingling, L. V. Zhigilei, B. J. Garrison, A. Koubenakis, J. Labrakis, S. Georgiou, Appl. Phys Lett. **78**, 1631 (2001).
[40] A. Koubenakis, J. Labrakis, S. Georgiou, Chem. Phys. Lett. **346**, 54 (2001).
[41] S. Georgiou, A. Koubenakis, M. Syrrou, P. Kontoleta, Chem. Phys. Lett. **270**, 491 (1997).
[42] C. Alba, L. E. Busse, D. J. List, C. A. Angell, J. Chem. Phys. **92**, 617 (1990).
[43] CRC Handbook of Chemistry and Physics, 75th ed., CRC Press, Boca Raton, FL (1995).
[44] [(a)] C. C. Han, Y.- L. W. Han, Y. C. Chen, Int. J. Mass Spectrom. **189**, 157 (1999).
[(b)] C. Focsa, J. L. Destombes, Chem. Phys. Lett. **347**, 390 (2001).
[45] S. Georgiou, A. Koubenakis, Chem. Rev. **103**, 349 (2003).
[46] R. Cramer, R. F. Hanglund Jr., F. Hillenkamp, Int. J. Mass Spectrom. Ion Processes **169-170**, 51 (1997).
[47] M. Karas, R. Krüger, Chem. Rev. **103**, 427 (2003).
[48] D. Eisenberg, A. D. McLachlan, Nature **319**, 199 (1986).
[49] T. D. Mark, M. Foltin, M. Kolibar, M. Lezius, P. Schreiber, Phys. Scr. I **53**, 43 (1994).
[50] A. Purice, J. Schou, P. Kingshott, M. Dinescu, Chem. Phys. Lett. **435**, 350 (2007).
[51] E. J. Houser, D. B. Chrisey, M. Bercu, N. D. Scarisoreanu, A. Purice, D. Colceag, C. Constantinescu, A. Moldovan, M. Dinescu, Appl. Surf. Sci. **252**, 4871 (2006).
[52] A. L. Mercado, C. E. Allmond, J. G. Hoekstra, J. M. Fitz-Gerald, Appl. Phys. A **81**, 591 (2005).
[53] A. Koubenakis, J. Venturini, S. Georgiou, Appl. Surf. Sci. **197-198**, 77 (2002).
[54] S. Georgiou, A. Koubenakis, P. Kontoleta, M. Syrrou, Chem. Phys. Lett. **260**, 166 (1996).
[55] S. Georgiou, A. Koubenakis, P. Kontoleta, M. Syrrou, Laser Chem. **17**, 73 (1997).
[56] S. Georgiou, A. Koubenakis, J. Labrakis, M. Lassithiotaki, J. Chem. Phys. **109**, 8591 (1998).
[57] A. Koubenakis, J. Labrakis, S. Georgiou, J. Chem. Soc. Faraday Trans. **94**, 3427 (1998).
[58] S. Georgiou, A. Koubenakis, J. Labrakis, M. Lassithiotaki, Appl. Surf. Sci. **127-129**, 122 (1998).
[59] G. C. Weaver, S. R. Leone, Surf. Sci. **328**, 197 (1995).
[60] G. C. Weaver, S. R. Leone, J. Phys. Chem. **100**, 4188 (1996).
[61] L. M. Cousins, S. R. Leone, J. Mater. Res. **3**, 1158 (1988).
[62] L. M. Cousins, S. R. Leone, Chem. Phys. Lett. **155**, 162 (1989).
[63] L. M. Cousins, R. J. Levis, S. R. Leone, J. Phys. Chem. **93**, 5325 (1989).
[64] Y. Song, P. Gardner, H. Conrad, A. M. Bradshaw, J. M. White, Surf. Sci. **248**, L279 (1991).
[65] Y. Tsuboi, K. Hatanaka, H. Fukumura, H. Masuhara, J. Phys. Chem. **98**, 11237 (1994).
[66] Y. Tsuboi, K. Hatanaka, H. Fukumura, H. Masuhara, J. Phys. Chem. A **102**, 1661 (1998).

[67] [(a)] O. Kokkinaki, M. Sc. Thesis, Univ. of Crete (2004).
[(b)] A. Koubenakis, Ph. D. Thesis, Univ. of Crete (2002).
[68] Y. G. Yingling, B. J. Garrison, Nucl. Instr. Meth. Phys. Rev. B **202**, 188 (2003).
[69] A. Rohlfing, C. Menzel, L. M. Kukreja, F. Hillenkamp, K. Dreisewerd, J. Phys. Chem. B **107**, 12275 (2003).
[70] P. Debenedetti, Metastable Liquids: Concepts and Principles, Princeton University Press: Princeton, NJ (1996).
[71] M. M. Martynyuk, Sov. Phys. Technol. Phys. **19**, 793 (1974).
[72] Y. P. Skripov, Metastable Liquids, John Wiley & Sons Inc., New York (1974).
[73] M. Blander, J. L. Katz, AlChE Journal **21**, 833 (1975).
[74] C. T. Avedisian, J. Phys. Chem. Ref. Data **14**, 695 (1985).
[75] K. Rah, B. C. Eu, Phys. Rev. E **68**, 051204 (2003).
[76] R. D. Goodwin, J. Phys. Chem. Ref. Data **18**, 1565 (1989).
[77] A. C. Tam, W. P. Leung, W. Zapka, W. Ziemlich, J. Appl. Phys. **71**, 3515 (1992).
[78] N. Do, L. Klees, A. C. Tam, P. T. Leung, W. P. Leung, J. Appl. Phys. **74**, 1534 (1993).
[79] O. Yavas, P. Leiderer, H. K. Park, C. P. Grigoropoulos, C. C. Poon, W. P. Leung, N. Do, A. C. Tam, Phys. Rev. Lett. **70**, 1830 (1993).
[80] O. Yavas, P. Leiderer, H. K. Park, C. P. Grigoropoulos, C. C. Poon, A. C. Tam, Phys. Rev. Lett. **72**, 2021 (1994).
[81] H. K. Park, C. P. Grigoropoulos, C. C. Poon, A. C. Tam, Appl. Phys. Lett. **68**, 596 (1996).
[82] K. Ishii, H. Nakayama, T. Okamura, M. Yamamoto, T. Hosokawa, J. Phys. Chem. B **107**, 876 (2003).
[83] O. Kokkinaki, A. Michalakou, A. Koubenakis, A. Michalakou, A. Koubenakis, J. Venturini, S. Georgiou, submitted.
[84] H. C. van de Hulst, Light Scattering by Small Particles, John Wiley & Sons Inc., New York (1981).
[85] V. Horneffer, R. Reichelt, K. Stupat, Int. J. Mass Spectr. **226**, 117 (2003).
[86] M. G. Kinsel, L. M. Preston-Schaffter, G. R. Kinsel, D. H. Russel, J. Am. Chem. Soc. **119**, 2534 (1997).
[87] F. Xiang, R. C. Beavis, Rapid Comm. Mass Spectr. **8**, 199 (1994).
[88] L. A. Crum, Nature **278**, 148 (1979).
[89] J. Frenkel, Kinetic Theory of Liquids, Dover Publications (1955).
[90] D. Sette, F. Wanderlingh, Phys. Rev. **125**, 409 (1962).
[91] F. E. Fox, K. F. Kertzfeld, J. Acoust. Soc. Am. **26**, 984 (1954).
[92] N. F. Bunkin, F. V. Bunkin, Sov. Phys. JETP **74**, 271 (1992).
[93] R.A. Wentzell, Phys. Rev. Lett. **56**, 732 (1986).
[94] R. D. Finch, J. Acoust. Soc. Am. **36**, 2287 (1964).
[95] M. P. Moody, P. Attard, Phys. Rev. Lett. **91**, 056104 (2003) and references therein.
[96] J. L. Parker, P. M. Claesson, P. Attard, J. Phys. Chem. **98**, 8468 (1994).
[97] S. Singh, J. Houston, F. van Swol, C. J. Brinker, Nature **442**, 526 (2006).
[98] M. Holmberg, A. Kühle, J. Garnaes, K. A. Mørch, A. Boisen, Langmuir **19**, 10510 (2003).
[99] T. S. Drakakis, G. Papadakis, K. Sambani, G. Filippidis, S. Georgiou, E. Gizeli, C. Fotakis, M. Farsari, Appl. Phys. Lett. **89**, 144108 (2006).
[100] [(a)] P. Marmottant, M. Versluis, N. de Jong, S. Hilgenfeldt, D. Lohse, Exp. Fluids **41**, 147 (2006).
[(b)] J. C. T. Eijkel, A. van den Berg., Microfl. Nanofl. **1**, 249 (2005).
[101] C.-M. Cheng, C.-H. Liu, Sens. Act. A **130-131**, 430 (2006).
[102] [(a)] K. Takahashi, K. Yoshino, S. Hatano, K. Nagayama, T. Asano, Proc. MEMS IEEE conf., 286 (2001).
[(b)] J. H. Tsai, L. Lin, IEEE/ ASME J. Micromech. Syst. **11**, 665 (2002).
[103] H. Y. Zheng, H. Liu, S. Wan, G. C. Lim, S. Nikumb, Q. Chen, Int. J. Adv. Manuf. Technol. **27**, 925 (2006).
[104] T. Kodama, A. Aoi, G. Vassaux, S. Mori, H. Morikawa, K.-C. Koshiyama, T. Yano, S. Fujikawa, Y. Tomita, Minimally Invasive Therapy **15**, 226 (2006).
[105] D. Perez, L. J. Lewis, P. Lorazo, M. Meunier, Appl. Phys. Lett. **89**, 141907 (2006).